Makara Journal of Technology

Volume 26 | Issue 2 Article 3

8-30-2020

Numerical Study of Paraffin Wax Melting in a Cavity with A Gradient of Hot Wall Inclination

Agus Dwi Korawan
Teknik Mesin, Sekolah Tinggi Teknologi Ronggolawe, Jawa Tengah 58315, Indonesia,
ad_korawan@yahoo.co.id

Recommended Citation

Korawan, Agus Dwi (2020) "Numerical Study of Paraffin Wax Melting in a Cavity with A Gradient of Hot Wall Inclination," *Makara Journal of Technology*: Vol. 26: Iss. 2, Article 3.
DOI: 10.7454/mst.v26i2.1472
Available at: https://scholarhub.ui.ac.id/mjt/vol26/iss2/3

Makara J. Technol. 26/2 (2022), 59–64
doi: 10.7454/mst.v26i2.1472

Numerical Study of Paraffin Wax Melting in a Cavity with A Gradient of Hot Wall Inclination

Agus Dwi Korawan*

Mechanical Engineering, Higher College of Technology Ronggolawe, Central Java 58315, Indonesia

*E-mail: ad_korawan@yahoo.co.id

Abstract

The melting of a phase change material (PCM) in a cavity with a gradient of hot wall inclination was simulated numerically using five models, namely, Model-A, Model-B, Model-C, Model-D, and Model-E with gradients of −2, −4, ∞, 4, and 2, respectively. The PCM was paraffin wax, which was melted using an enthalpy porosity technique with a pressure-based method. Model-A was found to be the best model. For the completion of the melting process, the models were assigned with the liquid fraction of 1. Model-A required the shortest time, followed by Model-B, Model-C, Model-E, and Model-D, respectively. Compared with Model-C, Model-A was 9.4% faster, Model-B was 3.8% faster, Model-D was 2.3% slower, and Model-E was 3.2% slower.

Abstrak

Studi Numerik Peleburan Parafin dalam Sebuah Rongga dengan Gradien Kemiringan Dinding Panas. Peleburan material berubah fasa dalam sebuah rongga dengan gradien kemiringan dinding panas telah disimulasikan secara numerik menggunakan lima model, yaitu Model-A, Model-B, Model-C, Model-D, dan Model-E dengan gradien kemiringan sebesar 2, 4, ∞, 4, dan 2. Material berubah fasa yang digunakan adalah parafin, proses peleburan menggunakan teknik *enthalpy porosity* dengan metode *pressure-based*. Model-A ditemukan sebagai model terbaik. Untuk penyelesaian proses peleburan, ditandai dengan fraksi cair bernilai 1. Model-A membutuhkan waktu tersingkat, diikuti oleh Model-B, Model-C, Model-E, dan Model-D. Dibandingkan dengan Model-C, Model-A 9,4% lebih cepat, Model-B 3,8% lebih cepat, Model-D 2,3% lebih lambat, dan Model-E 3,2% lebih lambat.

Keywords: hot wall inclination, melting, cavity, numerical, paraffin

1. Introduction

The thermal energy stored in latent heat is greater and thus more advantageous than that stored in sensible heat. Therefore, a latent heat storage system using a phase change material (PCM) is an effective way for storing thermal energy [1]. Paraffin is recommended as the PCM due to its good thermal properties [2], high latent heat, nonreactivity [3], latent heat of 176 kJ/kg, specific heat of 2.9 kJ/kg-K (liquid) and 2.7 kJ/kg-K (solid) [4], and low cost [5]. However, paraffin also has drawbacks, including low thermal conductivity [6], which result in a decrease in the overall performance of the heat storage system.

Several methods have been used to increase the heat transfer in the tube-and-shell model of heat storage with paraffin as the PCM. Some examples include installing internal fins [7], installing longitudinal and radial fins [8], changing the shape of the tube-and-shell to a nozzle-and-shell [9], and changing the shape of the tube-and-shell to combine-and-shell [10].

Different types of cavities and their effects have been studied because of their significant effect on the melting process. The position of the hot wall also plays an important role in the characteristics of the melting heat transfer. For instance, the melting rate and thermal heat stored for the vertical wall are greater than those for the horizontal wall during heating [11].

Visualization of paraffin melting shows that the process is initially dominated by conduction from the vertical wall to the solid paraffin. Fusion begins to occur at the liquid–solid interface parallel to the hot wall. Convection heat transfer becomes dominant because the hot paraffin liquid moves up parallel to the hot wall [12].

According to the Nusselt number during melting, conduction is the dominant mode in the initial melting stage, followed by a short transition. Afterward, convection dominates the entire melting phase, followed by weak convection at the last moment. Heat transfer has four stages: conduction, transition, strong convection, and weak convection [13].

Any increase in melting rate depends on the shape and orientation of the hot wall. Changing the shape of the hot wall from flat to wavy could increase the melting rate: the greater the amplitude of the hot wall wave, the greater the rate of melting [14].

Viscosity, conductivity, and differences in circulation also influence the melting process. Differences in these conditions are observed in four cases with different arrangements of two heat source–sink pairs [15].

This numerical study reported the melting process of PCM in a rectangular cavity with different gradients of hot wall inclination. The five types of models are shown in Figure 1. Model-A, Model-B, Model-C, Model-D, and Model-E had a gradient of hot wall inclination (m) of −2, −4, ∞, 4, and 2, respectively. The hot wall was at a constant temperature, and the other walls were in an adiabatic condition. Paraffin wax was used as the PCM. A numerical study was conducted to visualize the liquid–solid interface inside the melting paraffin wax. The stored energy and liquid fraction were analyzed to understand the influence of the hot wall gradient on the melting process. The Nusselt number was used to explain the stages of heat transfer.

2. Computational Method

ANSYS FLUENT software was used for this numerical study. The model was developed in a geometry subprogram of the systemic component of ANSYS, exported to the mesh program component for generation, and given a boundary of the required unit. Furthermore, the model was exported to FLUENT for problem solving.

The following were assumptions in this numerical study: (a) The thermophysical properties of paraffin are temperature dependent. (b) The liquid paraffin in the melt exhibits laminar flow. (c) The liquid paraffin is Newtonian. (d) The viscous dissipation is neglected. (e) The volume variation due to melting is neglected.

User Defined Functions were used to measure the density, thermal conductivity, and viscosity of the paraffin based on temperature. The hot wall was set at a constant temperature of 330 K, and the initial temperature of paraffin was 300 K. The adiabatic wall was set with a heat flux of 0. The SIMPLE scheme was used as a solution method, and the PRESTO scheme was adopted as the pressure correction equation. The First Order Upwind scheme was applied to solve the momentum and energy equations. The under-relaxation factors for the pressure, density, momentum, and energy were 0.3, 1, 0.7, and 1, respectively. The convergence absolute criterion for the continuity was set to 10-3, and that for the energy was set to 10-7. The time step for integrating the temporal derivatives was set to 0.1 s.

The enthalpy–porosity technique [7] was used as the model in which the liquid–solid interface was not explicitly tracked. Alternatively, the liquid fraction was tracked in every iteration based on the balance of the enthalpy.

The enthalpy of the material was computed as the sum of the sensible enthalpy, h, and latent heat, H [7]:

$$H = h + \Delta H, \tag{1}$$

$$h = h_{ref} + \int_{T_{ref}}^{T} C_p \, dT, \tag{2}$$

where h_{ref} is the reference enthalpy, T_{ref} is the reference temperature, and c_p is the specific heat at constant pressure.

The liquid fraction, β, can be defined as

$$\beta = 0 \quad if \quad T < T_{solidus}, \tag{3}$$

$$\beta = 1 \quad if \quad T > T_{liquidus}, \tag{4}$$

$$\beta = \frac{T - T_{solidus}}{T_{liquidus} - T_{solidus}} \quad if \quad T_{solidus} < T < T_{liquidus} \tag{5}$$

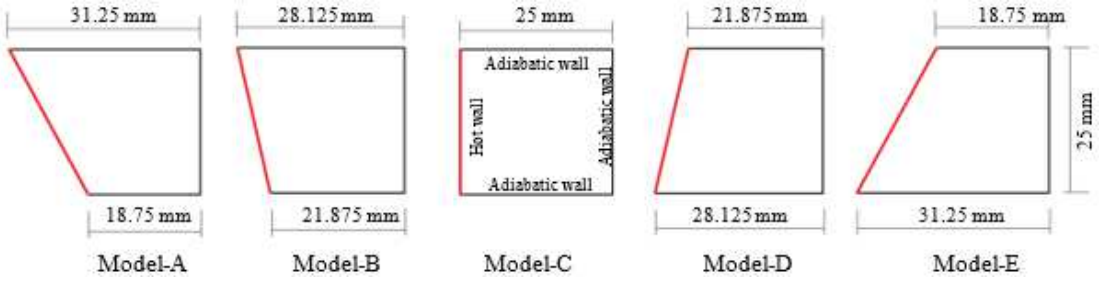

Figure 1. Models used for the Numerical Study

The latent heat content can now be written in terms of the latent heat of the material, *L*:

$$\Delta H = \beta L. \tag{6}$$

The latent heat content can vary between zero (for a solid) and *L* (for a liquid).

For melting problems, the energy equation can be written as

$$\frac{\partial}{\partial t}(\rho H) + \Delta.(\rho v H) = \Delta.(k\Delta T) + S, \tag{7}$$

where H is the enthalpy of the PCM, ρ is the density, v is the velocity, T is the temperature, k is the thermal conductivity, and S is the volumetric heat source term that is equal to 0 [1].

The thermophysical properties of the paraffin used in this study are listed in Table 1.

3. Validation of the Model

Model validation was conducted by comparing the numerical analysis (Model-C) to those reported by Arasu and Mujumdar [1]. Paraffin wax with 0% Al_2O_3 was used as the PCM. The vertical wall (hot and cold walls) was at a constant temperature, and the other two walls were adiabatic. The temperature of the hot wall was set at 330 K, and that of the cold wall was at 300 K. The initial temperature of the paraffin was 300 K, and the adiabatic wall was set with a heat flux of 0. The liquid fraction shown in Figure 2 illustrates reasonably good agreement.

Table 1. Thermophysical Properties of Paraffin Wax [1]

Property		
Density (kg/m^3)		$\frac{750}{0.001(T-319.15)+1}$
Thermal conductivity of solid (W/mK)	0.21	
Thermal conductivity of liquid (W/mK)	0.12	
Viscosity (Ns/m^2)		$0.001\exp(-4.25+\frac{1790}{T})$
Specific heat (J/kgK)	2890	
Latent heat (J/kg)	173400	
Liquidus temperature (K)	321	
Solidus temperature (K)	319	

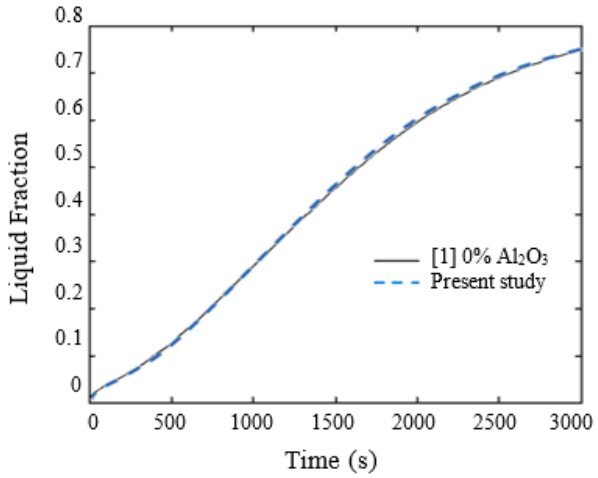

Figure 2. Comparison of Liquid Fraction in the Present Study and the Report of Arasu and Mujumdar [1] on Paraffin Wax with 0% Al_2O_3 Nanoparticles

4. Results and Discussion

The numerical simulation of paraffin melting for each model was conducted until all of the paraffin samples had completely melted. The liquid fraction, stored energy, and Nusselt number during the melting process were monitored. The results were presented and discussed to understand the influences of the gradient hot wall inclination on the melting process.

Figure 3 shows the contour of the velocity stream function, isotherms, and liquid–solid interface in Model-A at different melting times. In the early heating process, conduction was dominant as indicated by the isotherms lines parallel to the hot wall [2]. Given that the temperature of the hot wall was greater than that of the PCM melt temperature, the PCM melted extremely slowly along the hot wall.

Owing to the difference in the density between the high temperature of the liquid and the low temperature of the solid, the liquid was forced to move upward along the hot wall. Liquid flow was considered as the starting point of the changing isotherm, where the isotherm lines moved further in the upper part and convection gradually dominated.

Convection flow naturally moved upward, parallel to the hot wall, and then below, close to the liquid–solid interface. When the liquid moved upward, it accepted heat from the hot walls. When the liquid moved below, it transferred heat to the solid PCM so that melting occurred and the liquid temperature decreased continuously. Thus, the melting rate was more pronounced in the upper part of the container than in the lower part [2].

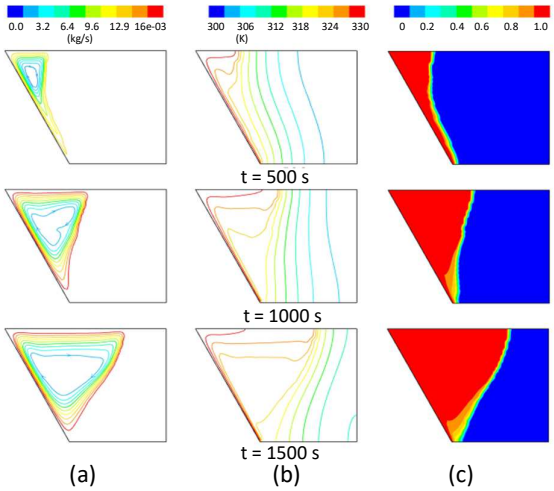

Figure 3. Contour of: (a) Velocity Stream Function, (b) Isotherms, and (c) Liquid–solid Interface

The comparison of the liquid–solid interface in Model-A to Model-E is shown in Figure 4. When t = 3000 s, the solid paraffin in Model-A had the least amount of residue among those in the other models, indicating the melting process of Model-A was the fastest. For Model-A and Model-E with the same length of the hot wall and opposing gradients, the speed of the melting process in Model-A was faster than that in Model-E. Similarly, the melting process of paraffin in Model-B was quicker than that in Model-D.

Figure 5 shows the evolution of the liquid–solid interface in the five models determined by combining seven images of the liquid–solid interface from each model at t = 500 s, 1000 s, 1500 s, 2000 s, 2500 s, 3000 s, 3500 s. Despite a slight difference in the curve, the patterns of the liquid–solid interface showed an overall similarity among all of the models. When the end of the liquid–solid interface was on the upper wall and moved from the left side to the right over time, the length of the liquid–solid interface increased. Alternatively, when the end of the liquid–solid interface was on the right wall and gradually moved from top to bottom, the length of the liquid–solid interface decreased. Therefore, changes in the length of this liquid–solid interface affect the value of the convection.

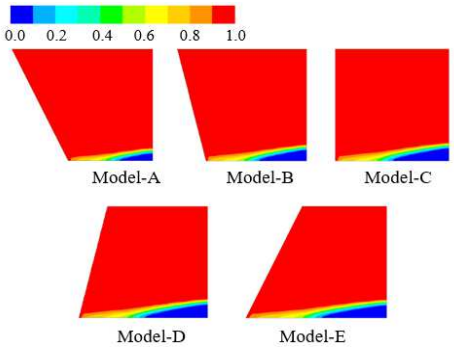

Figure 4. Comparison of the Liquid–solid Interface at t = 3000 s

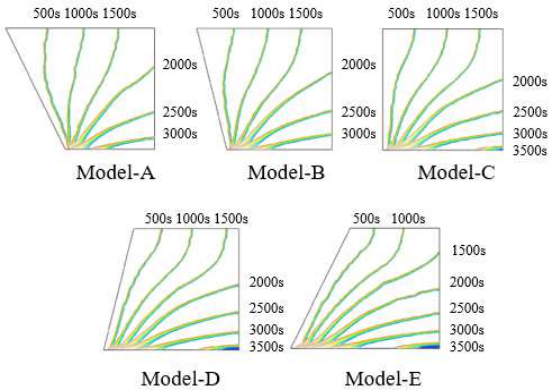

Figure 5. Evolution of the Liquid–solid Interface

The time necessary to achieve a liquid fraction of 1 in the five models during melting is shown in Figure 6. Despite having different values, all the models had the same patterns of liquid fraction. Until the end of the melting process, Model-A was the fastest, followed by Model-B, Model-C, Model-E, and Model-D. The required time to achieve the liquid fraction of 1 for all the models is presented in Table 2.

According to the comparison of the cases with the same length of the hot wall but the opposite gradient, the liquid fraction in Model-A was 12.3% faster than that in Model-E, and the liquid fraction in Model-B was 6.0% faster than that in Model-D. Therefore, despite the same length of the hot wall, the melting times will vary when opposite gradients are applied.

The total energy stored at t = 3000 s is presented in Table 3. Model-A stored the most energy, followed by Model-B, Model-C, Model-D, and Model-E. When the energy stored between Model-A and Model-E had the same length of the hot wall but opposite gradients, Model-A had 4.5% greater energy than Model-E. A similar trend occurred between Model-B (m = 4) and Model-D (m= −4); Model-B had 2.3% greater energy than Model-D. Therefore, a negative gradient increases the amounts of stored energy compared with a positive gradient.

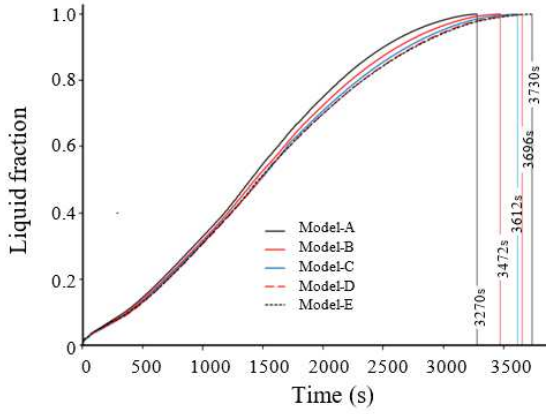

Figure 6. Liquid Fraction

Table 2. Required Time to Achieve A Liquid Fraction of 1

Model	Time (s)	Comparison with Model-C
A	3270	9.4% faster
B	3472	3.8% faster
C	3612	0
D	3696	2.3% slower
E	3730	3.2% slower

The surface Nusselt number on the hot wall is shown in Figure 7. The change in the shape of the Nusselt number indicates a different heat transfer mechanism in the melting process [3]. In the beginning of the melting process, the Nusselt number was extremely high, indicating that the liquid has yet to form via heat transfer conduction. In the later stage, the Nusselt number decreased when a layer of the liquid started to form. In this period, the thermal transfer modes were conduction and convection (Region 1). A slow increase subsequently occurred, indicating strong convection (Region 2). However, at a later stage, the Nusselt number decreased again, indicating diminished convection (Region 3). The Nusselt number during Transitions 1 and 2 varied for each model, and the transitions occurred at different times as presented in Table 4.

Figure 8 illustrates the time to Transition 1 and Transition 2, which is correlated with the liquid–solid interface. With time, the liquid–solid interface in Region 1 was relatively parallel to the hot wall, that in Region 2 was longer, and that in Region 3 was decreasing. In addition, some transitions occurred within the regions.

Table 3. Energy Stored

Model	Energy stored (J) at t = 3000 s	Comparison with Model-
A	159.02	3.2% higher
B	156.15	1.4% higher
C	154.00	0
D	152.63	0.8% smaller
E	152.12	1.2% smaller

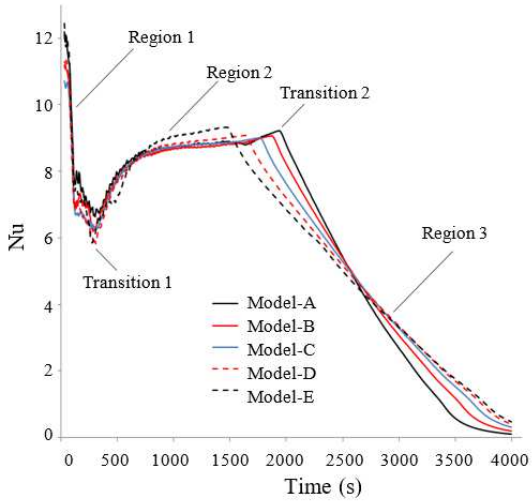

Figure 7. Surface Nusselt Number on the Hot Wall

Table 1. Nusselt Number

Model	Transition 1 (s)	Nu	Transition 2 (s)	Nu
A	302	6.65	1940	9.22
B	284	6.20	1874	9.08
C	310	6.25	1770	9.02
D	308	5.84	1640	9.09
E	276	5.86	1462	9.33

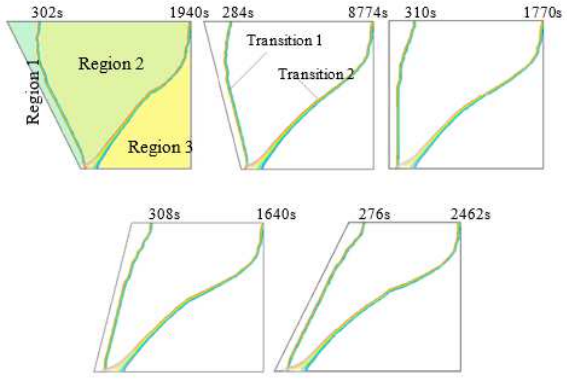

Figure 8. Region at the Liquid–solid Interface

All of the models had a short period of Region 1, indicating the heat transfer was changing faster than toward conduction than toward convection. The liquid flowed faster so that the convection heat transfer mode dominated quickly. Region 2 was longer, resulting in long strong convection. In Region 3, convection diminished because the liquid–solid interface was reduced.

5. Conclusions

For the completion of the melting process, Model-A is the fastest, followed by Model-B, Model-C, Model-E, and Model-D. A similar trend is observed for the stored energy, with Model-A storing the most energy.

According to the Nusselt number, Model-A has the shortest transition. Hence, convection occurs quickly and becomes strong for a long time.

References

[1] A. Sharma, V.V. Tyagi, C.R. Chen, D. Buddhi, Renew. Sustain. Energy Rev. 13/2 (2009) 318.
[2] K. Kavitha, S. Arumugam, Int. J. Renew. Energy Resour. 3 (2013) 1.
[3] B. Zalba, J.M. Marın, L.F. Cabeza, H. Mehling, Appl. Thermal Eng. 23/3 (2003) 251.
[4] A. Agarwal, R.M. Sarviya, Mater. Today Proc. 4/2 (2017) 779.
[5] M.M. Farid, A.M. Khudhair, S.A. K. Razack, S. Al-Hallaj, Energy Convers. Manag. 45/9–10 (2004) 1597.
[6] N. Soares, J.J. Costa, A.R. Gaspar, P. Santos, Energy Build. 59 (2013) 82.
[7] V. Shatikian, G. Ziskind, R. Letan, Int. J. Heat Mass Transf. 51/5–6 (2008) 1488.
[8] T.M. Hamdani, M. Irwansyah, Mahlia, Procedia Eng. 50 (2012) 122.
[9] A.D. Korawan, S. Soeparman, W. Wijayanti, D. Widhiyanuriyawan, Model. Simul. Eng. (2017).
[10] A.D. Korawan, S. Soeparman, W. Wijayanti, D. Widhiyanuriyawan, Model. Simul. Eng. (2017) 1.
[11] A.V. Arasu, A.S. Mujumdar, Int. Commun. Heat Mass Transf. 39/1 (2012) 8.
[12] N.S. Dhaidan, J.M. Khodadadi, T.A. Al-Hattab, S.M. Al-Mashat, Int. J. Heat Mass Transf. 66 (2013) 672.
[13] H. Shokouhmand, B. Kamkari, Exp. Therm. Fluid Sci. 50 (2013) 201.
[14] T. Kousksou, M. Mahdaoui, A. Ahmed, A.A. Msaad, Energy 64 (2014) 212.
[15] A. Ebrahimi, A. Dadvand, Alex. Eng. J. 54/4 (2015) 1003.